Interferometric Studies for the Annealing Effects on the Necking Deformation along Polypropylene Fibers

Hassan Mohamed El-Dessouky, Ph.D.[1,2], Ahmed A. Hamza[2], Ahmed E. Belal[3], T.Z.N. Sokkar[2], Khaled M. Yassien[3]

[1]University of Leeds, Leeds, United Kingdom
[2]Physics Department, Faculty of Science, Mansoura University, Egypt
[3]Faculty of Science, Aswan, South Valley University, Egypt

Corresponding Author:
H.M. El-Dessouky, Ph.D. email: texhed@leeds.ac.uk

ABSTRACT
An automated multiple-beam Fizeau fringes in transmission technique was used with a fiber-drawing device to detect necking deformation along polypropylene (PP) fibers axis under different conditions of annealing process. The refractive indices, refractive index profiles and crystallinity were calculated along the annealed PP fibers at different draw ratios. The annealing temperature controls the propagation of necking deformation along PP fibers axis that stretched at low draw ratios (D< 2). The necking deformations along PP fibers axis due to fast drawing process could be avoided when PP fibers were annealed at the temperature of 120^{o}C. Microinterferograms are given for illustrations.

INTRODUCTION
The optical anisotropy produces significant structural changes in such fibers for optimizing materials of much industrial interest. It is important technically to produce polymers with different characteristics, such as steel hardness and sponge softness, etc [1]. One of the most available techniques for changing the polymeric and physical structure is the annealing process. The effects of annealing increase drastically with temperature, but also depend on the time, which the sample is held at the annealing temperature [2-4].

The relation between the degree of crystallinity and the density of the polymer has great influence on the visco-elastic properties of crystalline polymers. Also, it is known that annealing and quenching at different conditions leads to changes in the density, crystallinity and optical parameters, etc. [2-4]. Many authors [5,6] have studied the molecular mechanisms that appear during the deformation of semi-crystalline polymers. The complexity of these deformations mechanisms is strongly related to the crystalline phase, which may be deformed by a range of mechanisms, such as slipping and twinning.

The mechanical behavior of polymers is closely linked in its amorphous and crystalline phases and their interfacial region. The main factor that controls its properties is the chain conformation in the solid state, which depends strongly on the crystallization and therefore on the thermo-mechanical history of the polymer [7]. The influence of mechanical behavior varies with annealing and measurement temperature [8]. The drawing and annealing treatment was used to improve the mechanical properties of polymer fibers [3]. Applying the mechanical stress of equal loads on the fibers, the mechanical properties would be improved by increasing the number of the tie chains in the amorphous regions and making uniform those lengths [4]. The structure, thermal and mechanical properties of polypropylene fiber reinforced random co-polypropylene composites have been studied with reference to fiber diameter [9].

When some polymers are drawn at low draw ratios, they deformed and showed a narrowing of the thickness (called necking) [10,11]. Necking is a smoothed jump in cross-sectional area of long and thin bars propagating with a constant speed. Cold-drawing of semi-crystalline polymers, such as polypropylene fibers, contain the initiation of local necking and the propagation of neck shoulders along the specimen [12]. Gent [13] related necking to the mechanism of unfolding chains in crystalline blocks and transferring them into amorphous phase with consequent orientation. Abo-El-Maaty et al. [14] studied the formation of defects on drawn polypropylene fibers. Their investigations showed that during the drawing of these PP fibers there are longitudinal defects developed within these fibers.

Interferometric techniques are accurate methods for studying opto-mechanical properties of polymer fibers [15,16]. Hamza et al. [15] used the fiber drawing device to detect and avoid dynamically the necking deformation, which occurs along un-annealed polypropylene fibers axis stretched with

low draw ratios using multiple-beam interferometric technique. El-Mohager and Heymans [8] observed the localized deformation and the appearance of necking deformation that propagates along annealed polymer sample at the temperatures of 23, 40 and 120°C.

In this paper a tensile-drawing device attached to the system for producing multiple-beam Fizeau fringes in transmission is used to investigate the influence of annealing on the necking deformation along the axis of polypropylene fibers. Some optical and structural parameters of un-annealed and annealed PP fibers are calculated at different draw ratios.

THEORETICAL CONSIDERATIONS

Refractive index and its profile of fibers

Multiple-beam Fizeau fringes is one of the most accurate techniques for the measurements of the optical properties of fibers [17]. For the determination of the mean refractive index for light vibrating parallel and perpendicular to the fiber axis, we use the following formula [18]:

$$n^i = n_L \pm \frac{F^i \lambda}{2bA} \quad (1)$$

Where i denotes the state of light polarization (parallel $\parallel$ or perpendicular $\perp$ to the fiber axis), n_L is the refractive index of the immersion liquid, F is the area enclosed under the fringe shift inside the fiber, λ is the wavelength of the monochromatic light used, b is interfringe spacing, A is the fiber cross sectional area and the sign ($\pm$) depends on the direction of the fringe shift inside the fiber.

The refractive index profile taking the refraction of the fiber into consideration can be calculated using the following equation [19]:

$$\frac{\lambda Z_Q}{b} = \sum_{j=1}^{Q-1} 2n_j[K1 - K2]^{1/2} + 2n_Q K3 - n_0 K4 \quad (2)$$

Where K1, K2, K3 and K4 are given by

$$K1 = \sqrt{[R-(j-1)a]^2 - (d_Q n_o / n_j)^2}$$

$$K2 = \sqrt{(R-ja)^2 - (d_Q n_o / n_j)^2}$$

$$K3 = \sqrt{[R-(Q-1)a]^2 - (d_Q n_o / n_Q)^2}$$

$$K4 = \sqrt{R^2 - d_Q^2} + \sqrt{R^2 - X_Q^2}$$

Where j is the layer number, a is the layer thickness ($a = R/Q$), R is the fiber radius, Q is the number of layers, n_o is the refractive index of the immersion liquid, n_j is the refractive index of the layer *jth*, d_Q is the distance between the incident beam and the fiber center, X_Q is the distance between the emerging beam and the fiber center, Z_Q is the fringe shift corresponding to the point X_Q in the multiple-beam interference pattern (microinterferogram).

Density and degree of crystallinity

The density is one of the most important physical parameters that reflect the thermal effect on materials. It is strongly related with refractive index of fibers by the following equation [20];

$$\rho = K \frac{(n_{iso}^2 - 1)}{(n_{iso}^2 + 2)} \quad (3)$$

Where K=3.14 for *PP* fibers [20] and n_{iso} is the isotropic refractive index and given by $n_{iso}=1/3(n^{\parallel}+2n^{\perp})$.

Depending on the density, the degree of crystallinity χ for *PP* fibers can be determined using the following equation [21]:

$$\chi = \frac{\rho - \rho_a}{\rho_c - \rho_a} \times 100 \quad (4)$$

Where ρ_c and ρ_a are the densities of the crystalline and amorphous regions, ρ_c=0.950 *g/cm*^{3} and ρ_a =0.936 g/cm^3 for *PP* fibers [22].

EXPERIMENTAL SET-UP AND TECHNIQUES

Standard polypropylene (PP) fibers were taken as spun. The initial diameter of these fibers was nearly equal 86 μm. Samples of PP fibers are mounted (free ends) on glass rods then entered into an electric oven to raise their temperature. The temperature is adjusted to the relevant temperature (60, 90 and 120°C). The samples are annealed for one hour, then left to cool in air at room temperature 30°C.

A tensile-drawing device [23] attached to the system for producing multiple-beam Fizeau fringes in transmission (*Figure 1*) is used to investigate the necking deformation along PP fibers under different conditions of annealing (T= 30, 60, 90 and 120°C). A sample of certain length from PP fibers is fixed at its ends with two clamps of drawing system and put on the lower optical flat of the liquid wedge interferometer (1). This wedge interferometer [24] consists of two circular optical plates with diameter 35mm, 7mm thickness and flatness ± 0.01 μm. The inner surface of each optical plate is coated with highly reflecting, partially transmitting sliver layer.

The two optical plates are put in a special holder. Few drops of an immersion liquid (having refractive index close to that of the fiber) are dropped on the silvered face of the lower optical flat. The fiber is then immersed in the liquid and its ends fixed. The upper flat is introduced to form the silvered liquid wedge. The gab thickness and the wedge angle of the interferometer are adjusted by using three screws in order to get sharp fringes across the fiber. The shape of the fringe shift and its direction with respect to the apex of the interferometer depends on the relative values of the refractive index of the immersion liquid and the fiber.

The fiber-drawing system as shown in *Figure 1* is transferred to the optical interference system, where the wedge interferometer is fixed on the microscope stage (2). The motion of this stage can be controlled via micrometer screw (3). A parallel beam (4) of polarized monochromatic light is used to illuminate this liquid wedge interferometer, which is adjusted in such a way that the fiber axis is exactly perpendicular to the interference fringes in the liquid region. When straight-line fringes crossed the fiber they suffered a shift Z due to the difference between the refractive index of the immersion liquid and the mean refractive index of the fiber.

The obtained fiber image (microinterferogram) was captured using the CCD camera (5) and computerized unit. This image (6) is digitized directly via the digitizer frame grabber that is built in the computer. The digitized image is recorded on the computer storage media. The micrometer screw (3) moves the drawing system, to obtain the microinterferograms along the fiber axis at different draw ratios and for different annealing temperatures.

RESULTS AND DISCUSSION

The PP fibers were drawn at low draw ratios (D<2) with fast drawing process [15]. The refractive indices of the used immersion liquids are 1.5022, 1.5054, 1.5070 and 1.5091 for un-annealed PP fibers at a temperature T= 30°C and for annealed PP fiber at temperatures T= 60, 90 and 120°C, respectively. Monochromatic light of wavelength (λ=546.1 nm) was used.

Figures 2-5 show the obtained microinterferograms in the parallel and perpendicular direction of un-annealed and annealed PP fibers samples at temperatures T= 60, 90 and 120°C, respectively, for the draw ratios D= 1.2, 1.4, 1.6 and 1.8. *Figure 2* illustrates that the necking deformation propagates along the annealed PP fiber axis stretched with fast drawing at draw ratios D= 1.2, 1.4, 1.6 and 1.8.

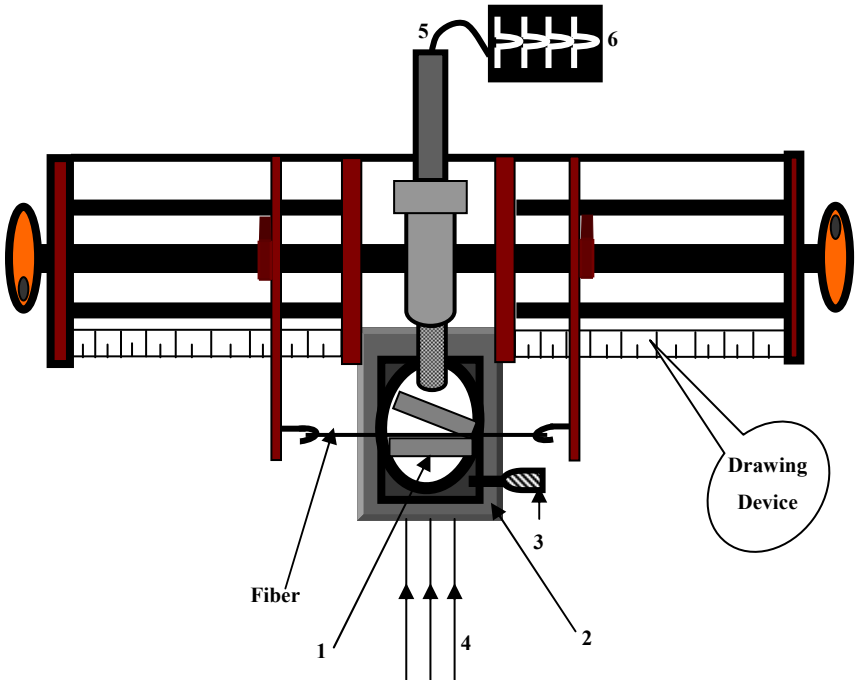

FIGURE 1. Schematic diagram of the modified drawing device attached with Fizeau system where: 1- wedge interferometer, 2- microscope stage, 3-micrometer screw, 4-parallel beams, 5- CCD camera and 6- image of the fiber [23] .

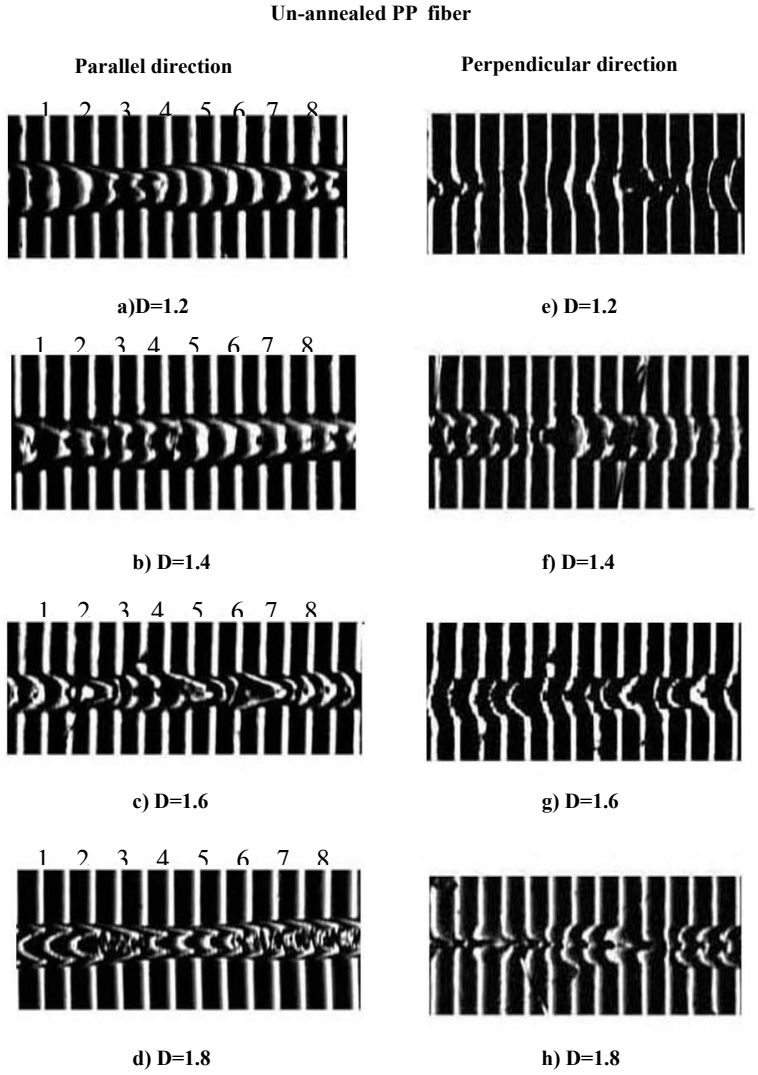

FIGURE 2. The obtained microinterferograms for light vibrating parallel and perpendicular to the fiber axis of un-annealed PP fiber showing necking deformation at draw ratios D=1.2,1.4, 1.6 and 1.8.

From these microinterferograms (*Figure 2*) it is clear that, there are random and significant changes in the fiber fringe shifts and thickness along the PP fibers due to the necking deformation [11,15].

For an annealed PP fiber at T=60°C, the occurrence of necking deformation nearly decreased along the fiber axis by increasing draw ratio and disappeared at draw ratio D=1.8 [*Figure 3*(d,h)]. At this draw ratio the fiber fringe shifts and thickness became uniform in shapes along the PP fiber. By increasing annealing temperature (T= 90°C) the occurrence of necking deformation along the fiber axis disappeared at draw ratios D= 1.6 and 1.8 [*Figure 4*(c,d,g and h)]. For an annealed PP fiber at T =120°C, the PP fiber slightly affected by a small necking deformation along fiber axis at draw ratio D=1.2. By increasing draw ratio (1.4, 1.6 and 1.8) the propagation of necking deformation disappears along the fiber axis at draw ratio D=1.2. By increasing draw ratio (1.4, 1.6, and 1.8) the propagation of necking deformation disappears along the fiber axis [*Figure 5* (b,c,d,f,g and h)]. In these cases there is a smooth change in the fiber fringe shifts and thickness with the draw ratio. The above results illustrate that necking deformation is detected along the annealed PP fiber axis [8]. Also, it is obvious that by increasing annealing temperature the propagation of necking deformation along the PP fiber axis decreases. This necking deformation is nearly avoided.

Quantitatively the mean refractive index $n^{\|}$ of PP fibers are calculated at each fringe shift along the fiber axis with the aid of the microinterferograms of *Figures 2-5* using *Eq. (1)*. *Tables I-IV* give the variation of refractive indices along the fiber axis for

Annealed PP fiber at T=60 °C

Parallel direction

Perpendicular direction

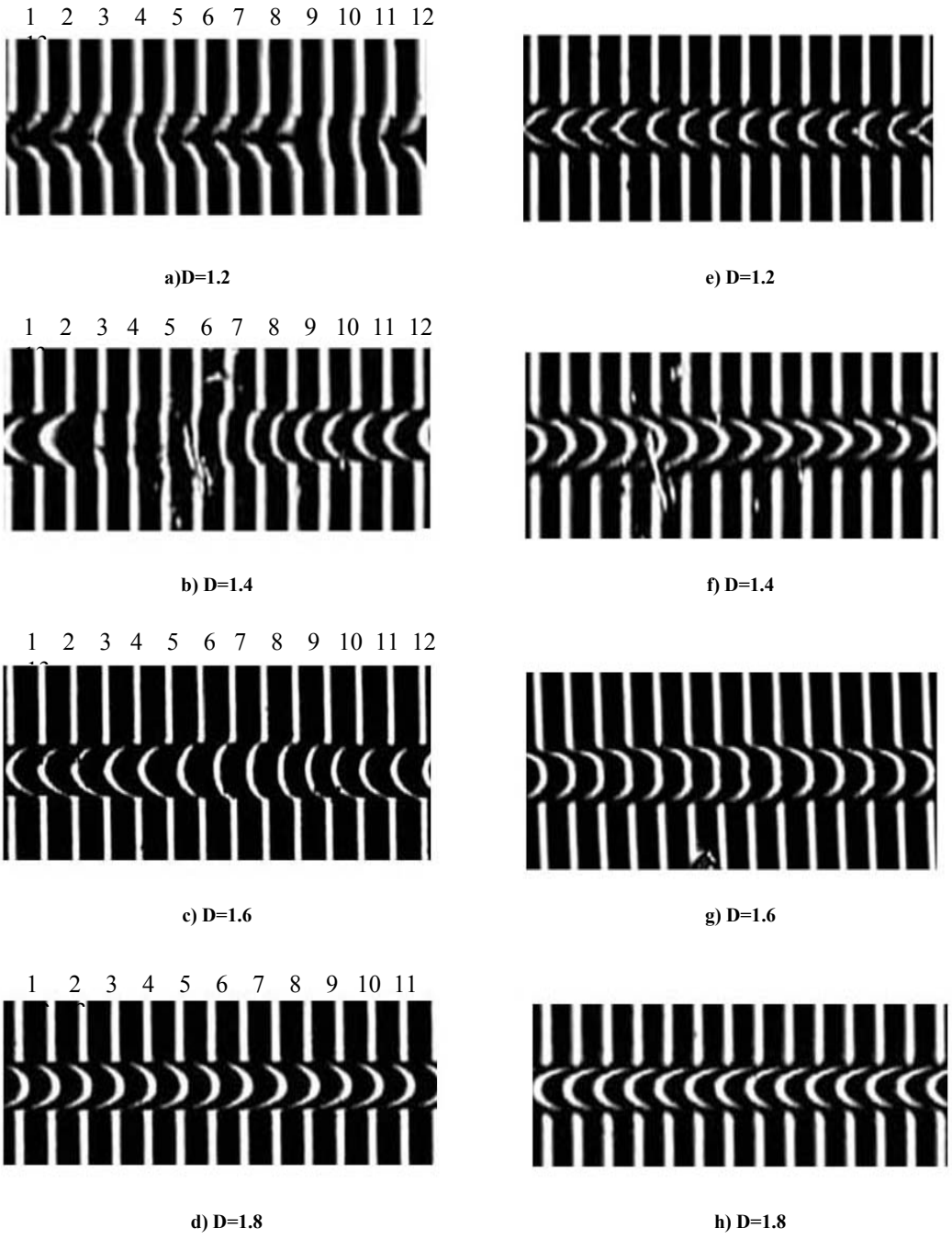

FIGURE 3. The obtained microinterferograms for light vibrating parallel and perpendicular to the fiber axis of annealed PP fiber at temperature T= 60°C for draw ratios D= 1.2, 1.4, 1.6 and 1.8.

Annealed PP fiber at T=90°C

Parallel direction **Perpendicular direction**

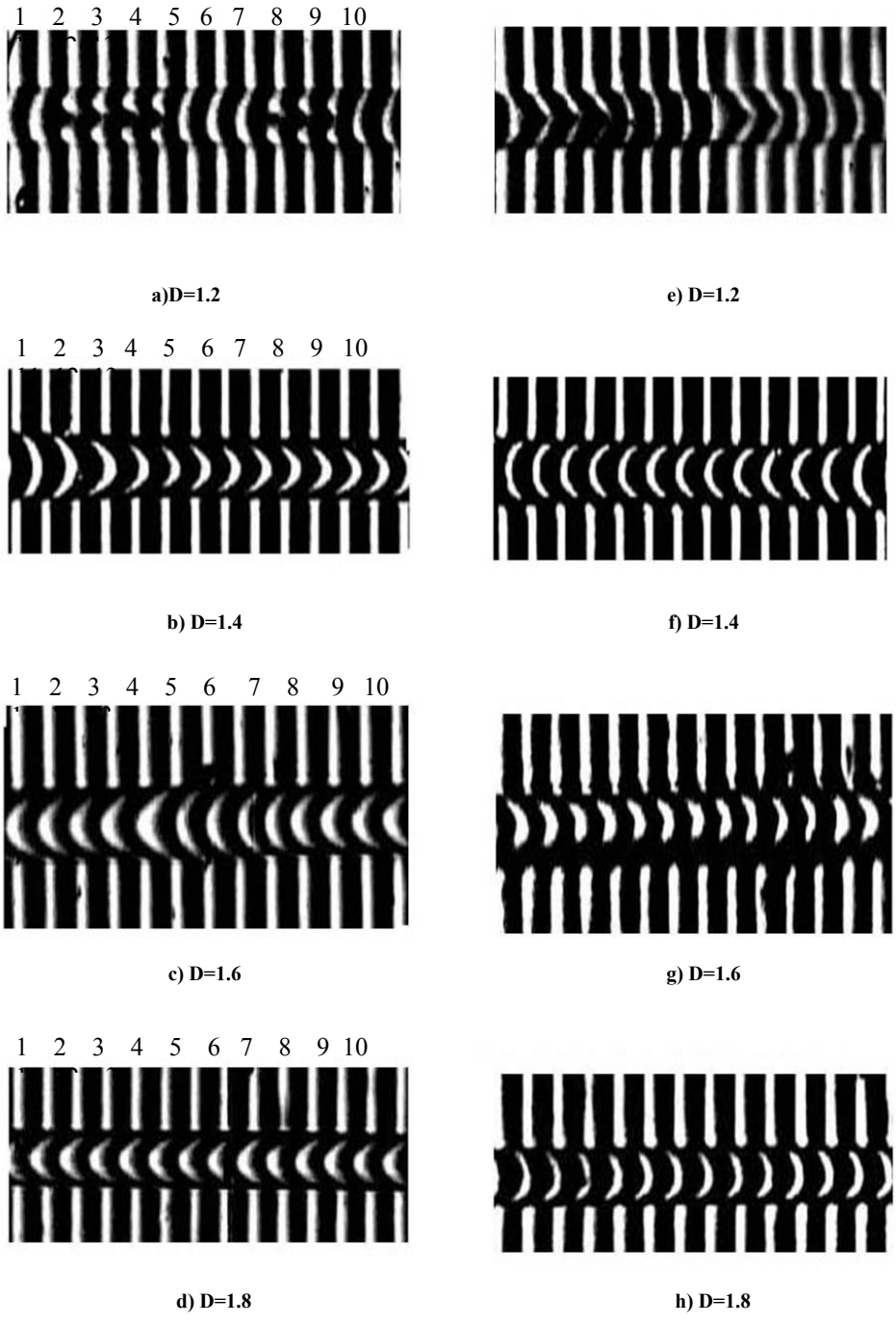

FIGURE 4. The obtained microinterferograms for light vibrating parallel and perpendicular to the fiber axis of annealed PP fiber at temperature T= 90°C for draw ratios D= 1.2, 1.4, 1.6 and 1.8.

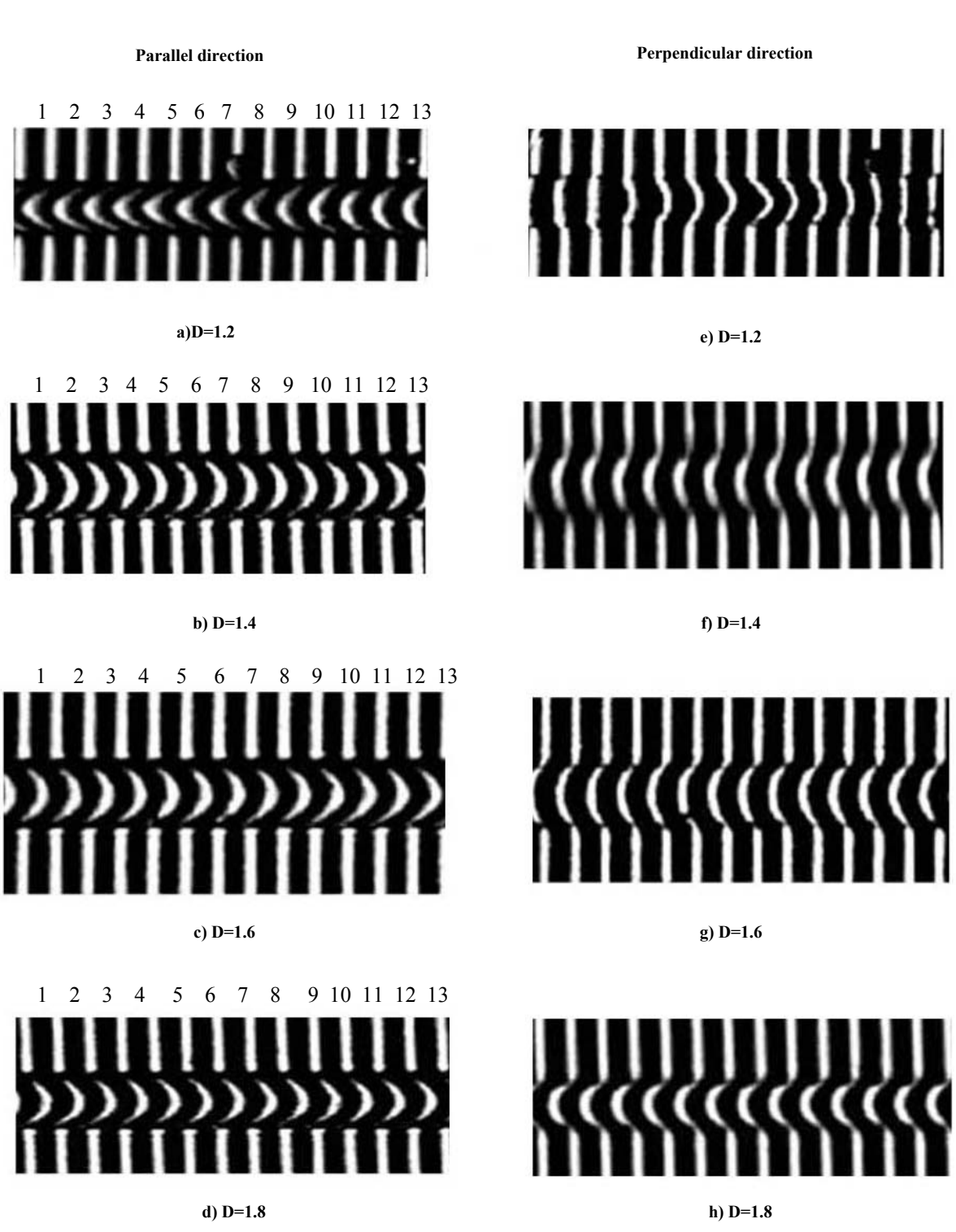

FIGURE 5. The obtained microinterferograms for light vibrating parallel and perpendicular to the fiber axis of annealed PP fiber at temperature T= 120°C for draw ratios D= 1.2, 1.4, 1.6 and 1.8.

un-annealed and annealed PP fibers at temperatures T= 60, 90 and 120°C, respectively, for draw ratios (D= 1.2, 1.4, 1.6 and 1.8). It is obvious from *Table I* that values of refractive indices vary along the fiber axis at different draw ratios (D= 1.2, 1.4, 1.6 and 1.8) for un-annealed PP fiber. The refractive indices of PP fibers have small and high values at different regions along the fiber axis at each draw ratios. The high values of refractive indices due to that thickness of fiber at these regions are thinner than other regions, which their values of refractive indices are small. These due to those fibers are drawn in some regions more than other regions. These variations confirm the propagation of necking deformation along the PP fiber axis. For annealed PP fiber at temperature equals 60°C, *Table II* shows that there are significant changes in the values of refractive index $n^{\parallel}$ along the fiber axis at different draw ratios (D= 1.2, 1.4, 1.6). These variations result from the variation of thickness along the fiber axis. Also, it is clear from this table that at draw ratio D=1.8, there are no variation in the values of $n^{\parallel}$ along the fiber axis. This due to the fact that the fiber has constant thickness and the necking is avoided at this draw ratio. By increasing annealing temperature, there are no variation in the values of $n^{\parallel}$ along the fiber axis at draw ratios D=1.4, 1.6 and 1.8 for annealed PP fiber at 120°C (*Table IV*). These results show that the necking deformation is nearly avoided by increasing annealing temperature and draw ratio. Also, *Table IV* shows that the values of $n^{\parallel}$ increases with increasing of draw ratio (D=1.4, 1.6, 1.8) [16,23].

To confirm the influence of annealing on necking deformation along stretched PP fibers axis, the principal refractive index profiles for the parallel direction are measured using image-processing steps [25] with the aid of *Eq. (2)*. The fringe shifts in the microinterferograms for parallel direction [*Figures 2-5*] are remarked to be easy for identification. The refractive index profiles are calculated for each fringe shift of microinterferograms given in *Figures 2-5*. *Figures 6-9* show the refractive index profiles along the fiber axis of un-annealed and annealed PP fibers at temperatures T= 60, 90 and 120°C, respectively, for draw ratios (D= 1.2, 1.4, 1.6 and 1.8). From these figures, the un-annealed PP fibers show that there are significant variations in the refractive index profiles at different positions along the fiber axis for draw ratios = 1.2, 1.4, 1.6 and 1.8 [see *Figure 6*]. The variety in these profiles is present due to the occurrence of necking deformation along the fiber axis.

For annealed PP fiber at T= 60°C, by increasing draw ratio up to (D=1.8) the changes in the refractive index profiles along the fiber axis decreased [*Figure 7*]. At this draw ratio D=1.8 there are no variations in the fringe shifts along the fiber axis, hence the refractive index profile for each fringe shift has the same behavior as shown in *Figure 6(d)*. By increasing annealing temperature up to 120°C the deformations in the fringe shifts along the fiber disappears at draw ratios D= 1.4, 1.6 and 1.8. Therefore there are no variations in the refractive index profiles along the fiber axis at these draw ratios [*Figure 9(b,c,d)*]. The refractive index profiles of PP fibers at different annealing temperatures throw light on the influence of annealing on the necking deformation along the fiber axis.

In quantitative details on the influence of annealing on the structural deformation of PP fibers, the crystallinity is calculated along the fiber axis with the aid of *Eq. (4)* and is given in *Figure 10*.

TABLE I The variation of refractive indices along the fiber axis which showing the effect of necking deformation on un-annealed PP fibers at draw ratios (D= 1.2, 1.4, 1.6 and 1.8).

Distance along the fiber x 10^2 □m	**Refractive index**			
	Draw ratio D= 1.2	Draw ratio D= 1.4	Draw ratio D= 1.6	Draw ratio D= 1.8
0.71	1.5049	1.5061	1.5045	1.5041
1.42	1.5052	1.5136	1.5045	1.5041
2.13	1.5052	1.5077	1.5045	1.5076
2.84	1.5056	1.5044	1.5061	1.5076
3.55	1.5056	1.5044	1.5061	1.5076
4.26	1.5056	1.5044	1.5061	1.5052
4.97	1.5056	1.5044	1.5061	1.5052
5.68	1.5060	1.5044	1.5061	1.5076
6.39	1.5060	1.5057	1.5078	1.5198
7.1	1.5052	1.5057	1.5078	1.5185
7.81	1.5052	1.5077	1.5078	1.5185
8.52	1.5056	1.5077	1.5078	1.5263
9.23	1.5056	1.5077	1.5078	1.5207

TABLE II The variation of refractive indices along the fiber axis for annealed PP fibers at temperature T= 60ºC, for draw ratios (D= 1.2, 1.4, 1.6 and 1.8) and showing the stability of refractive index along the fiber axis at draw ratio D= 1.8.

Distance along the fiber x 10^2 □m	**Refractive index**			
	Draw ratio D= 1.2	Draw ratio D= 1.4	Draw ratio D= 1.6	Draw ratio D= 1.8
0.71	1.5075	1.5090	1.5100	1.5110
1.42	1.5070	1.5090	1.5100	1.5110
2.13	1.5055	1.5090	1.5100	1.5110
2.84	1.5057	1.5080	1.5090	1.5110
3.55	1.5070	1.5055	1.5070	1.5110
4.26	1.5070	1.5055	1.5070	1.5110
4.97	1.5070	1.5055	1.5070	1.5110
5.68	1.5070	1.5055	1.5070	1.5110
6.39	1.5050	1.5057	1.5072	1.5110
7.1	1.5052	1.5060	1.5080	1.5110
7.81	1.5052	1.5070	1.5090	1.5110
8.52	1.5070	1.5090	1.5100	1.5110
9.23	1.5070	1.5090	1.5100	1.5110

TABLE III The variation of refractive indices along the fiber axis for annealed PP fibers at temperatures T= 90ºC, for draw ratios (D= 1.2, 1.4, 1.6 and 1.8) and showing the stability of refractive index along the fiber axis at draw ratio D= 1.6, 1.8.

Distance along the fiber x 10^2 □m	**Refractive index**			
	Draw ratio D= 1.2	Draw ratio D= 1.4	Draw ratio D= 1.6	Draw ratio D= 1.8
0.71	1.5085	1.5095	1.5115	1.5128
1.42	1.5075	1.5105	1.5115	1.5128
2.13	1.5075	1.5110	1.5115	1.5128
2.84	1.5075	1.5120	1.5115	1.5128
3.55	1.5075	1.5130	1.5115	1.5128
4.26	1.5085	1.5130	1.5115	1.5128
4.97	1.5085	1.5130	1.5115	1.5128
5.68	1.5085	1.5130	1.5115	1.5128
6.39	1.5070	1.5130	1.5115	1.5128
7.1	1.5070	1.5130	1.5115	1.5128
7.81	1.5070	1.5130	1.5115	1.5128
8.52	1.5085	1.5120	1.5115	1.5128
9.23	1.5085	1.5110	1.5115	1.5128

TABLE IV The variation of refractive indices along the fiber axis for annealed PP fibers at temperature T= 120ºC, for draw ratios (D= 1.2, 1.4, 1.6 and 1.8) and showing the stability of refractive index along the fiber axis at draw ratio D= 1.4, 1.6, 1.8.

Distance along the fiber x 10^2 □m	**Refractive index**			
	Draw ratio D= 1.2	Draw ratio D= 1.4	Draw ratio D= 1.6	Draw ratio D= 1.8
0.71	1.5120	1.5150	1.5172	1.5185
1.42	1.5130	1.5150	1.5172	1.5185
2.13	1.5130	1.5150	1.5172	1.5185
2.84	1.5135	1.5150	1.5172	1.5185
3.55	1.5140	1.5150	1.5172	1.5185
4.26	1.5150	1.5150	1.5172	1.5185
4.97	1.5135	1.5150	1.5172	1.5185
5.68	1.5135	1.5150	1.5172	1.5185
6.39	1.5130	1.5150	1.5172	1.5185
7.1	1.5130	1.5150	1.5172	1.5185
7.81	1.5120	1.5150	1.5172	1.5185
8.52	1.5120	1.5150	1.5172	1.5185
9.23	1.5120	1.5150	1.5172	1.5185

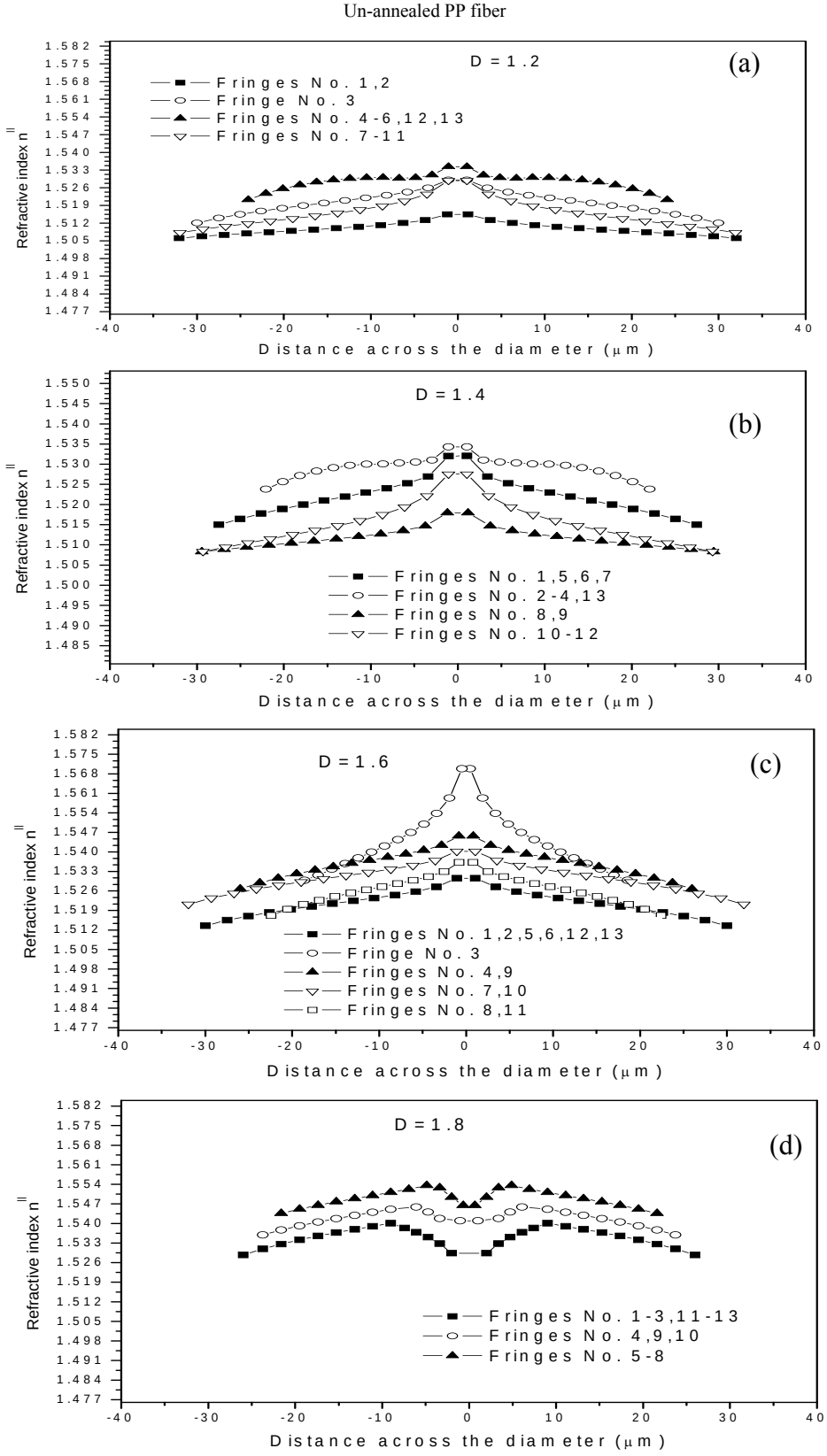

FIGURE 6. The refractive index profiles of $n^{\|}$ showing necking deformation along the fiber axis of un-annealed PP fiber at draw ratios D= 1.2, 1.4, 1.6 and 1.8.

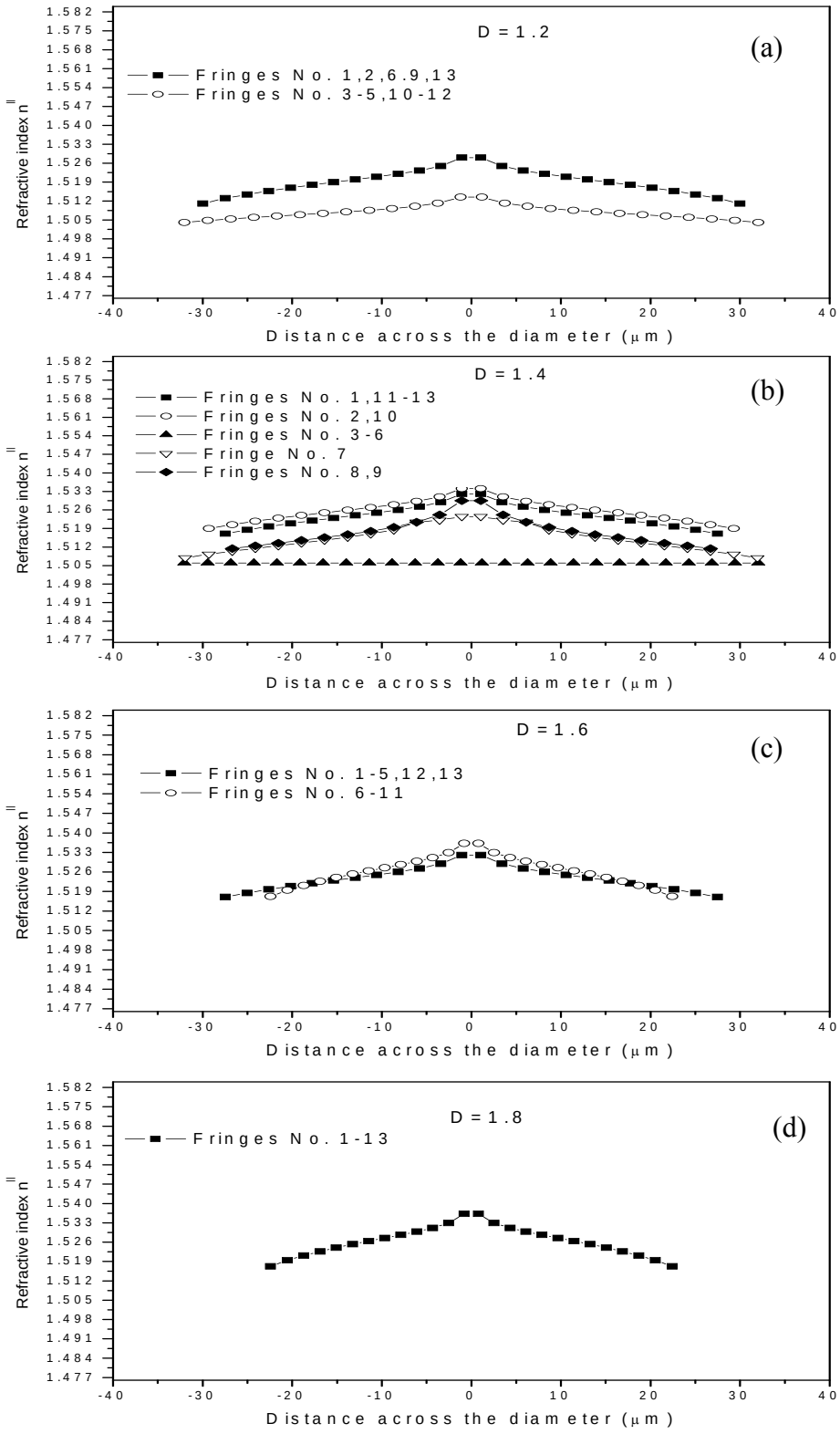

FIGURE 7. The refractive index profiles of $n^{\parallel}$ along the fiber axis of annealed PP fiber at temperature T= 60ºC for draw ratios D= 1.2, 1.4,1.6 and 1.8 and showing the staple of refractive index profile along the fiber axis at draw ratio D= 1.8.

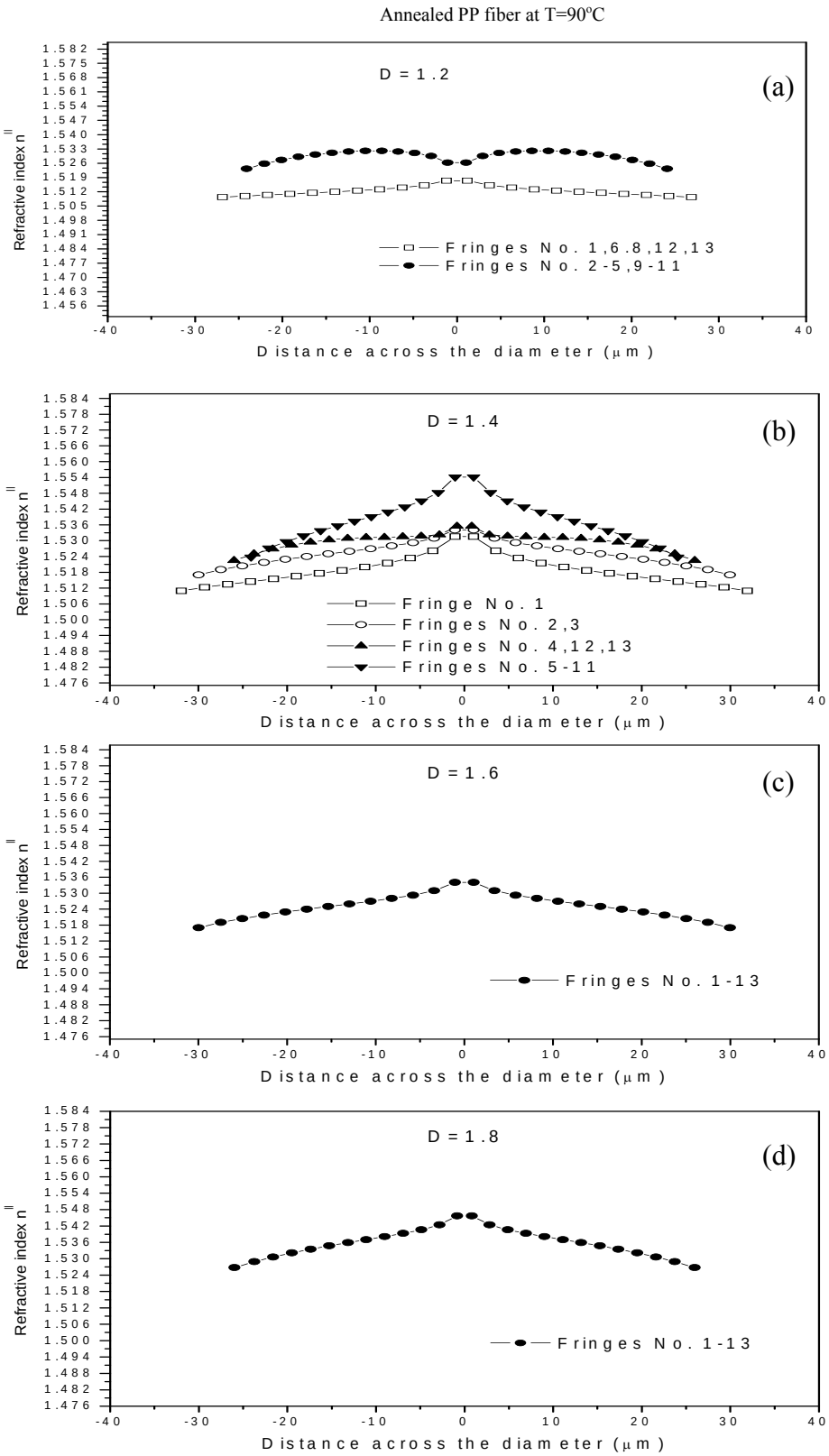

FIGURE 8. The refractive index profiles of $n^{\parallel}$ along the fibers axis of annealed PP fiber at temperature T=90ºC for draw rations D=1.2, 1.4, 1.6, and 1.8 and showing the staple of refractive index profile along the fiber axis at draw ratios D=1.6, 1.8.

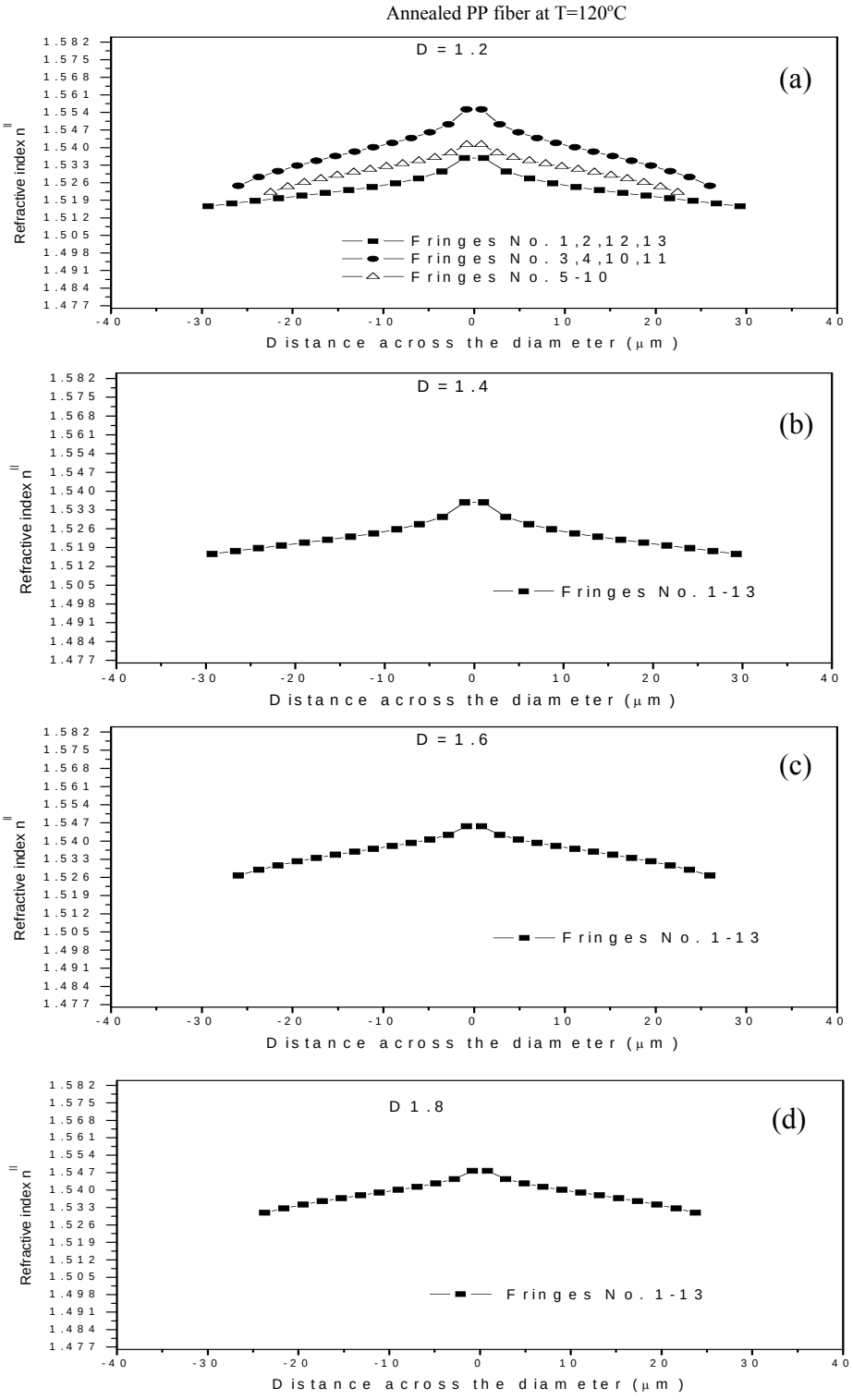

FIGURE 9. The refractive index profiles of $n^{\parallel}$ along the fiber axis of annealed PP fiber at temperature T= 120°C for draw ratios D= 1.2, 1.4,1.6 and 1.8 and showing the staple of refractive index profile along the fiber axis at draw ratio D= 1.4, 1.6, 1.8.

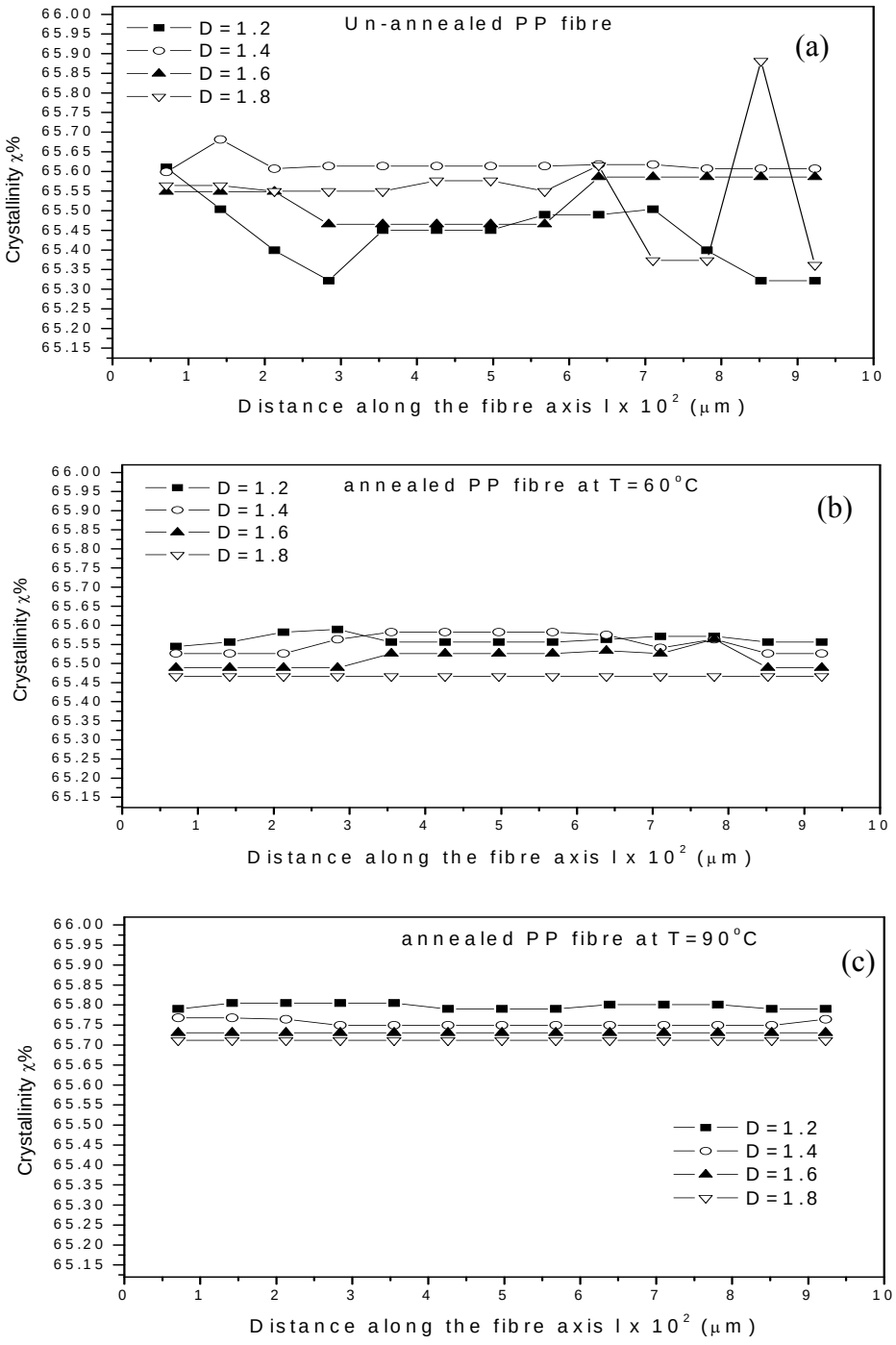

FIGURE 10. The crystallinity χ along the fiber axis of un-annealed and annealed PP fibers at temperatures T= 60 and 90°C for draw ratios D= 1.2, 1.4, 1.6 and 1.8.

The changes in orientation are accompanied by change of crystallinity due to the drawing process. This indicates mass redistribution within the fiber chains. Also, this indicates the change in density [26]. The crystallinity is almost important because the crystalline component is always of higher refractive index than the amorphous regions, regardless of whether the latter is glassy or rubbery [27].

Figure 10(a-c) shows the crystallinity along the fiber axis for un-annealed and annealed PP fibers at temperatures T= 60, 90 and 120°C, respectively, for draw ratios (D= 1.2, 1.4, 1.6 and 1.8). It is clear from this figure that there are variations in the value of crystallinity along the fiber axis for un-annealed PP fiber at different draw ratios [see *Figure 10(a)*]. For annealed PP fibers at temperature 60°C, these

variations decreased by increasing draw ratio [*Figure 10(b)*]. For annealed PP fibers at T=90^{o}C, the crystallinity has the same value along the fiber axis and has a smooth change at draw ratios D=1.4, 1.6 and 1.8 [*Figure 10(c)*]. Also this figure illustrates that the values of crystallinity increase by increasing annealing temperature. The increase of crystallinity may be due to the reduction of amorphous orientation by the chain relaxation [21]. *Figure 10* shows that the degree of crystallinity is lower for un-annealed fibers than for annealed samples. The crystallization in polymeric materials is usually described in terms of a nucleation and growth model [28]. The error in measuring refractive index n, refractive index profiles and crystallinity using multiple-beam technique are ±0.0007 [17].

The above results of microinterferograms, principal refractive index $n^{\|}$, refractive index profiles and crystallinity can evaluate quantitatively the effect of annealing on the necking deformation along PP fibers axis. These above results can be discussed qualitatively as follows:

At room temperature when PP fibers are drawn in the case of fast drawing the neck zones are formed, along the fiber axis, at mechanical weak bonds within the fiber structure. These neck zones are formed due to microscopic inhomogeneities and a large extent for the oriented polymer molecules [10]. For un-annealed PP fibers the necking deformation propagates along the fiber axis at draw ratios from D=1.2 to D=1.9. This is due to the excess of heating rate at necking positions than the limit of flowing temperature of the molecular chains [15,29,30]. By increasing temperature of annealing for PP fibers, the occurrence of necking deformation along fiber axis decreased. The thermal process increases the mobility of the chains and the axial mobility of the microfibrils. It also changes the crystalline and amorphous parts in fibers, where the crystallized areas increase the high modulus of rigidity, elasticity and ultimate tensile stress of fibers, whereas the amorphous areas gives the fibers flexibility, recovery, elongation and swelling. At different temperatures of annealing the material becomes more fragile and chain mobility increases, even inside the crystallites since they are able to crystallize at these temperatures [8]. By increasing draw ratio and annealing temperature the orientation of amorphous chains improved because the crystalline orientation factor increased [4]. Also at these conditions the crystalline orientation increased rapidly at small draw ratios and reached plateau at higher draw ratios [31]. The little necking deformation that appears in annealed PP fibers at the temperature 60^{o}C may be due to the presence of more defects, and an easy localization of deformation, although the crystals are large [8]. For annealed PP fibers at temperature 90^{o}C the necking deformation nearly disappears during fast drawing process. Hence we recommend that the annealing of PP fiber around 90^{o}C for one hour is a good heat treatment to avoid the propagation of necking deformation along the fiber axis stretched at low draw ratios (D<2).

CONCLUSION

A fiber drawing device attached to the system for producing Multiple-beam Fizeau fringes in transmission is used to detect necking deformation along polypropylene (PP) fibers axis under different conditions of annealing process. The microinterferograms clearly identify the variations in the thickness and fringe shifts along the fiber axis due to the necking mechanism for un-annealed and annealed PP fibers.

The refractive indices, refractive index profiles and crystallinity of PP fibers have small and high values at different regions along the fiber axis at each draw ratio for un-annealed PP fibers. These variations are due to the fact that those fibers are drawn in some regions more than other regions. The measured optical and structural properties such as refractive indices, refractive index profiles and crystallinity illustrate the influence of annealing on the propagation of necking deformation along PP fibers axis.

For annealed PP fibers, by increasing temperature of annealing, the occurrence of necking deformation along fiber axis decreases. For the annealed PP fibers at temperatures 90 and 120^{o}C the necking deformation nearly disappears during fast drawing process. Hence we recommend an annealing treatment around 100^{o}C for one hour would be required to avoid the propagation of necking deformation along the low drawn PP fibers.

REFERENCES

[1] Zbigniew K. W., ch. 7, "Formation of Synthetic Fibers", Gordon and Breuch Science Publishers, New York, (1977).

[2] Decandia F. and Vittoria, V., J. Poly. Sci. Phys. Ed., 23 (1985) 1217.

[3] Suzuki A., Chen Y. and Kunugi T., Polymer, 39 (1998) 5335.

[4] Suzuki A., Murata H. and Kunugi T., Polymer, 39 (1998) 1351.

[5] Gent A. N. and Madan S. J., Polymer Sci.: Part B: Polym. Phy., 27 (1989) 1529.

[6] Peterlin A., Colloid and Polymer Sci. 265 (1987) 357.

[7] Rault J., Semi-crystalline polymers, In: Plastic deformation of amorphous and semi-crystalline materials. Ed. Escaig B, G'sell C., Les editions de Physique. (1982) 313.

[8] El-Mohager B. E. and Heymans N., Polymer, 42 (2001) 7017.

[9] Houshyar S. and Shanks R., Journal of Macromolecular Materials and Engineering, 288 (2003) 599.

[10] Sova M., Raab M. and Sližová M., J. Mater. Sci. 28 (1993) 6516.

[11] Mabrouk M.A., Polymer Testing 21 (2002) 653.

[12] Kontou E. and Farasoglou P., J. Mater. Sci., 33 (1998) 147.

[13] Gent A. N., Rubber Chem. Technol., 69 (1996) 59

[14] Abo El Maaty M. I., Bassett D. C., Olley R. H., Dobb M. G., Tomka J. G. and Wang I.-C., Polymer, 37 (1996) 213.

[15] Hamza A. A., Sokkar T. Z. N., El-Farahaty K A., EL-Morsy M. A. M. and EL-Dessouky H. M., Optics and Laser Technology, 37 (2005) 532.

[16] Hamza A. A., Sokkar T. Z. N., El-Farahaty K A. and EL-Dessouky H. M., Journal of Applied Polymer Science, 95(2005) 647.

[17] Barakat N. and Hamza A. A., "Interferometry of Fibrous Materials", Adam Hilger, Bristol, (1990).

[18] Hamza A. A., Text. Res. J. 50 (1980) 731.

[19] 19. Hamza A. A., Sokkar T. Z. N., Ghander A. M., Mabrouk M A.and Ramadan W. A., Pure. Appl. Opt., 4 (1995) 161.

[20] de Vries J., Bonnebat C. and Beautemps J., J. Appl. Polym. Sci., Symp., 58 (1977) 109.

[21] Lebourvellec G. and Beautemps J., J. Appl. Polym. Sci., 39 (1990) 329.

[22] Tager A. "Physical Chemistry of Polymers" MIR, Moscow, (1978).

[23] Hamza A. A., El-Farahaty K. A. and Helaly S. A., Optica Applicata, 18, No. 2 (1988) 133.

[24] Barakat N. and El-Hennawi H. A., Text. Res. J., 41 (1971) 391.

[25] Hamza A. A., Sokkar T. Z. N., Mabrouk M. A., and El-Morsy M. A., J.Appl. Poly. Sci., 77 (2000) 3099.

[26] Dusanc-Prevorsek Z., J. Polym. Sci. Part A-2, 4(1966) 63.

[27] Jekins A. D. Polymer Science, A materials Science Hand Book, Vol. 1, Ch. 4 and 7. Amsterdam: North-Holland, (1972).

[28] Turnbull D. and Fisher J. C., J. Chem. Phys., 17 (1949) 71; Polymer, 15 (1974) 283.

[29] Jasbrich M., Diacik I. and Faser U., Textile Techn., 18 (1967) 331

[30] Kobayashi J., Okajama S. and Narita A., J. Appl. Polym. Sci., 11 (12) (1967) 2515.

[31] Murthy N. S., Gray R. G., Correale S. T. and Moore R. A., Polymer, 36 (1995) 3863.

AUTHOR'S ADDRESS

Hassan Mohamed El-Dessouky, Ph.D.
University of Leeds
Department of Textile Industries
School of Design
Leeds, LS2 9JT
UNITED KINGDOM

T.Z.N. Sokkar; Ahmed A. Hamza
Mansoura University
Physics Department
Faculty of Science
EGYPT

Ahmed E. Belal; Khaled M. Yassien
South Valley University
Faculty of Science
Aswan
EGYPT